



Prediction and performance analysis of compression index of multiple-binder-treated soil by genetic programming approach

Kennedy C. Onyelowe^{1,2} · Ahmed M. Ebid³ · Light Nwobia¹ · Lam Dao-Phuc⁴

Received: 17 April 2021 / Accepted: 10 May 2021
© The Author(s), under exclusive licence to Springer Nature Switzerland AG 2021

Abstract

The use and its advantage in overcoming time and equipment needs of an evolutionary prediction technique known as the genetic programming have been studied using unsaturated sample of soft soil treated with multiple binders. The soil classified as weak and highly plastic was stabilized and multiple experiments were conducted to measure the effect of the dosages of the treatment on the selected properties. The geotechnics of the exercise showed that the studied parameters substantially improved with increased proportion of hybrid cement (HC) and nanostructured quarry fines (NQF). These measured selected properties were further deployed to predict the compression index of the soil. The prediction operation proposed four-model equation by the degree of importance, sensitivity and influence of the independent parameters. This shows eventually that plasticity index has the greatest sensitivity on the compression behaviour of clay soils. The performance analysis shows that the models have very low error with model trial 4 presented in Eq. 7: $C_C^{GP} = \frac{(I_p - HC \cdot NQF) \left[\left(\frac{\sigma_{part}}{\sigma_{max}} \right)^{NQF} \right]^{(I_p/w_{max})}}{\ln(w_{max} + 3.0)}$, showing the least error with more consideration for the influence of more of the selected variables. It also exhibited the highest degree of determination. Generally, GP has proven to be flexible, fast and able to predict models for engineering problems for use in design and performance study.

Keywords Nanostructured quarry fines · Genetic programming (GP) · Performance analysis and error analysis · Soft computing · Compression index · Unsaturated soil

✉ Kennedy C. Onyelowe
kennedychibuzor@kiu.ac.ug; konyelowe@gmail.com

Ahmed M. Ebid
ahmed.abdelkhaleq@fue.edu.eg;
ahmad_m_ebid@yahoo.com

Light Nwobia
nwobia.light@mouau.edu.ng

Lam Dao-Phuc
lamdp@utt.edu.vn

- ¹ Department of Civil Engineering, Michael Okpara University of Agric, Umudike, Nigeria
- ² Department of Civil and Mechanical Engineering, Kampala International University, Kampala, Uganda
- ³ Department of Structural Engineering, Faculty of Engineering and Technology, Future University, Cairo, Egypt
- ⁴ Structure-Materials for Highway Section, Faculty of Civil Engineering, University of Transport Technology, Hanoi, Vietnam

Abbreviations

| | |
|-----------------|--|
| HC | Hybrid cement (%) |
| NQF | Nanostructured quarry fines (%) |
| C_C | Coefficient of curvature |
| C_u | Coefficient of uniformity |
| δ_{max} | Maximum dry density (g/cm ³) |
| w_{max} | Optimum moisture content (%) |
| δ_{part} | Partial maximum dry density (g/cm ³) |
| w_L | Liquid limit (%) |
| I_p | Plasticity index (%) |
| C_C^S | Skempton's compression index |
| C_C^{GP} | Genetic programming proposed compression index |

Introduction

Emerging trends in civil engineering have necessitated the adoption of various evolutionary computation (EC) techniques for the analyses and predictions of functional parameters towards solving multiple geoenvironmental problems [9, 14, 15, 16, 17, 18, 24]. The obsolescence of conventional

methods triggered by their limitations in terms of low computational strength and incorporation of certain unrealistic traditional assumptions has further glorified the benefit of utilizing machine learning algorithms in the field of civil engineering. Genetic programming (GP) is one of those evolutionary computation techniques, inspired by the natural evolution of genetic processes that has the capacity of approximating linear and/or nonlinear relationship within a random dataset while continuously seeking for an optimal solution and avoiding local minima errors during operations among the set of scattered programs [6, 15, 26]. As a technique that imposes slight modifications to the robust genetic algorithms (GA) to achieve a more desirable result, GP which is anchored by the Darwinian theory of natural selection has performed excellently well for the prediction of solutions in the simple and complex domains [3, 19]. In addition to their general abilities to automatically learn from input and output data to perform their predictions, GP has the exceptional capability of generating independent practical prediction equations, making it a more versatile technique than many other evolutionary computation (EC) or computational intelligence (CI) techniques such as support vector machines (SVM), artificial neural networks (ANN), fuzzy inference systems (FIS), adaptive neuro-fuzzy inference systems (ANFIS), adaptive boot algorithms (ABA) and decision tree (DT) [3, 12, 13, 16, 17].

Despite gaining significant research impetus within the last few decades, many research attentions have been directed to the use of GP in performing various prediction studies in the areas of structural engineering, geotechnical engineering, water resources engineering and even beyond. For instance, in the area of water engineering, Azamathulla and Zahiri [13] performed discharge prediction in compound channels using GP. In their investigation, they successfully derived a precise dimensionless equation for prediction of flood discharge. By employing laboratory and field stage–discharge datasets from channels with compound sections, Zahiri and Hashemi [1] predicted the individual flow discharge of the main channel by applying gene expression programming (GEP) and further compared performance with traditional divided channel methods. In addition to justifying its applicability in the area of structural engineering, Gandomi and Alavi [11] employed GP and multilinear expression programming (MEP) for the prediction of shear strength of reinforced concrete columns and the hysteretic energy demand in steel moment-resisting frames and useful/reliable results were achieved. Their results proved to be adequate as prediction equations for all cases investigated were successfully developed without incorporating simplifying modelling assumptions. GP has also been applied to model the performance of structural concrete under controlled condition throughout time [14]. Another powerful potential of the robust GP technique is its usage in performing virtual

reality simulations. It has been reported by Shaw et al. [28] that GP proved excellent for use in the conceptual design of frame structures and the visualization of results using VRML/X3D to produce virtual reality simulations. Because of its ability to mirror a tree structure, enabling mathematically complex expressions to be evaluated and simulated with ease, the GP has readily been implemented using various programming languages that naturally embody tree-like structures mechanism. The use of GP has also been reflected in highway engineering-associated predictions. In this situation, Mazari and Rodriguez [20] developed a model used in the prediction of international roughness index (IRI), which is a fundamental performance indicator in pavement roughness.

Critical long-term drivers of geotechnical dynamics such as urbanization, technological advancement and population growth have propelled the evolution of recent research trends in the field of geotechnical engineering that incorporate the use of evolutionary computations, particularly GP in predicting and modelling the behaviours of various soil parameters [27]. In fact, the past 30 years have seen increasingly rapid advances in systems and techniques of soil improvement-related prediction using GP. Alavi and Sadrossadat [3] confirmed the usability of the prediction equations obtained via GP as reliable and accurate technique when modelling the bearing capacity of shallow foundations resting on a soil mass.

The compression index (C_c) is an important soil mechanical property determined by conducting one-dimensional consolidation test (oedometer test). The oedometer test is a technique employed to determine consolidation characteristic of low-permeability soils when subjected to vertical load [23]. Conventional method of determining compression index via oedometer test is cumbersome and expensive [22, 23]. Due to its complexity in the use of conventional methods for estimation, Ibrahim et al. [23] obtained compression index by executing plasticity index. In their own contribution to providing and validating more robust approaches for compression index prediction, Benbouras et al. [22] performed a comparative study using K-fold cross-validation technique by utilizing several models of multilayer neural networks (MNN), genetic programming (GP) and multiple regression analysis (MRA). Although he reported the artificial neural network (ANN) to perform better than the other employed evolutionary computation techniques, the ANN models could not offer precise prediction equations which can be useful for subsequent predictions.

By and large, most studies on the application of GP in geotechnical engineering have dominantly been carried out in a small number of areas, particularly on soil improvement inspired by various compaction techniques, as well as on soil settlement predictions [2, 9, 21, 25, 26]. In addition, no significant research has been found that surveyed the prediction

of compression index (CI) based on a genetic programming technique. Based on the discussed advantages offered by the GP technique of evolutionary computation, this study explores the use of genetic programming (GP), which falls in line with the algorithmic structure presented by Vidal and Huynh [30] in Fig. 1 in predicting the compression index of soil in an unsaturated condition treated with multiple binders of hybrid cement generated by activating rice husk ash with alkali materials and nanostructured quarry fines generated by completely pulverizing quarry dust to fineness. This work proves the potential of machine learning techniques in modelling and predicting geotechnical parameters in a stabilization protocol where pozzolanic binders, which satisfy the positions of ASTM C618 [4] and Onyelowe et al. [18], were obtained from solid waste recycle and reuse technique for a cleaner and greener earthwork exercise.

Materials and methods

Materials

Clayey soil was obtained from the location as shown in the map in Fig. 2, and basic studies show that it possessed the following characteristics: percentage passing 0.075-mm size sieve, 45%, natural moisture content, 14%, liquid limit, 66%, plastic limit, 21%, plasticity index, 45%, swelling potential, 23%, AASHTO classification, A-7-6, maximum dry density, 1.25% obtained at an optimum moisture content of 16% with a high degree of expansion. This reference soil was used in this research work. The above data show that the soil is expansive, weak, highly plastic and lacks the structural and mechanical qualities to be considered as a foundation material. Hence, rice husk ash (RHA) was generated through direct combustion of rice husk collected from local

rice mills and farm areas in Abakaliki. In order to improve the binding ability of RHA, 5% hydrated lime by weight of the RHA was blended with the RHA and allowed for 24 h. This exercise gave rise to hydrated lime-activated rice husk ash (HARHA), which was utilized in varying percentages to modify the soil, and tests were conducted to produce values for the model. Nanostructured quarry fines (NQF) was generated by pulverizing quarry dust (QD) and passing it through 200-nm size sieve. The size distribution and morphology of the soil and the rice husk ash are presented in Figs. 3, 4 and 5, respectively.

It can be seen in Fig. 4 that RHA exhibits gel-like porous-valve structure at a magnification level of 100 μm . Additionally, the presence of bigger voids could be observed in the SEM micrograph, which illustrates the light-weight structure and porous structure of the agricultural waste. Similarly, the SEM image in Fig. 5 depicts a laminar structure with dispersive, larger and thinner clay platelets. The smectites are seen to conform plate-like structures with the presence of thin hairline cracks. Additionally, the aggregates are mostly arranged in a face-to-face contact style in Fig. 5. Figure 6 presents the UV-Vis spectrophotometric nanograph of nanostructured quarry fines, which shows the absorbance of the materials and its ability to form homogenous blend with soil and RHA. Lastly, Fig. 7 shows the compaction characteristics of the lateritic soil sample.

Methods and collected database

The requirements of the British Standard International (BSI) [7] were adopted in conducting preliminary tests on the materials for the purpose of identification and characterization. Under the above design conditions, the particle size analysis, compaction, Atterberg limits, specific gravity, cohesion and the angle of internal friction were conducted. In order to determine the morphology and oxides composition of the composite binder materials (RHA, HC and NQF), the scanning electron microscopy (SEM) and the x-ray fluorescence (XRF) exposures were carried out in accordance with the ASTM E1621-13 [5], and in order to achieve reliable and precise results, the samples were prepared and mixed to high homogeneity and the results were observed and recorded. Also, the UV-Vis spectrophotometer test was conducted on the NQF to determine the absorbance of the nanoparticle exposure of the material. Further, the multiple-binder stabilization exercise of the soil was conducted in accordance with the requirements of the [8] and multiple data points were generated for varying dosages of HC and NQF between 0 and 12% by weight of dry soil. The studied parameters of the treated soil were coefficient of curvature, coefficient of uniformity, maximum dry density (g/cm^3), optimum moisture content (%), partial maximum dry density (g/cm^3), liquid

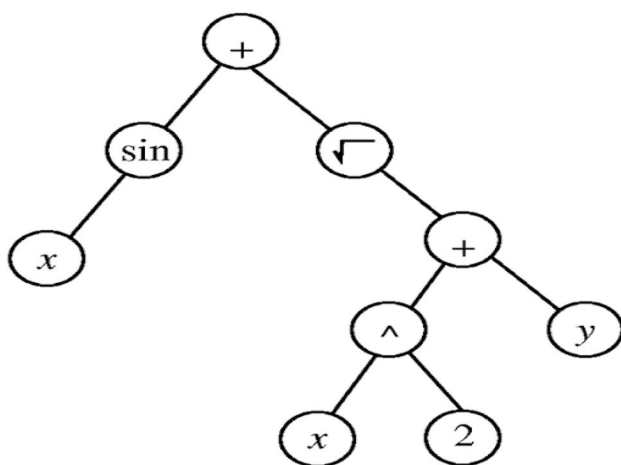


Fig. 1 Algorithmic structure of genetic programming [30]

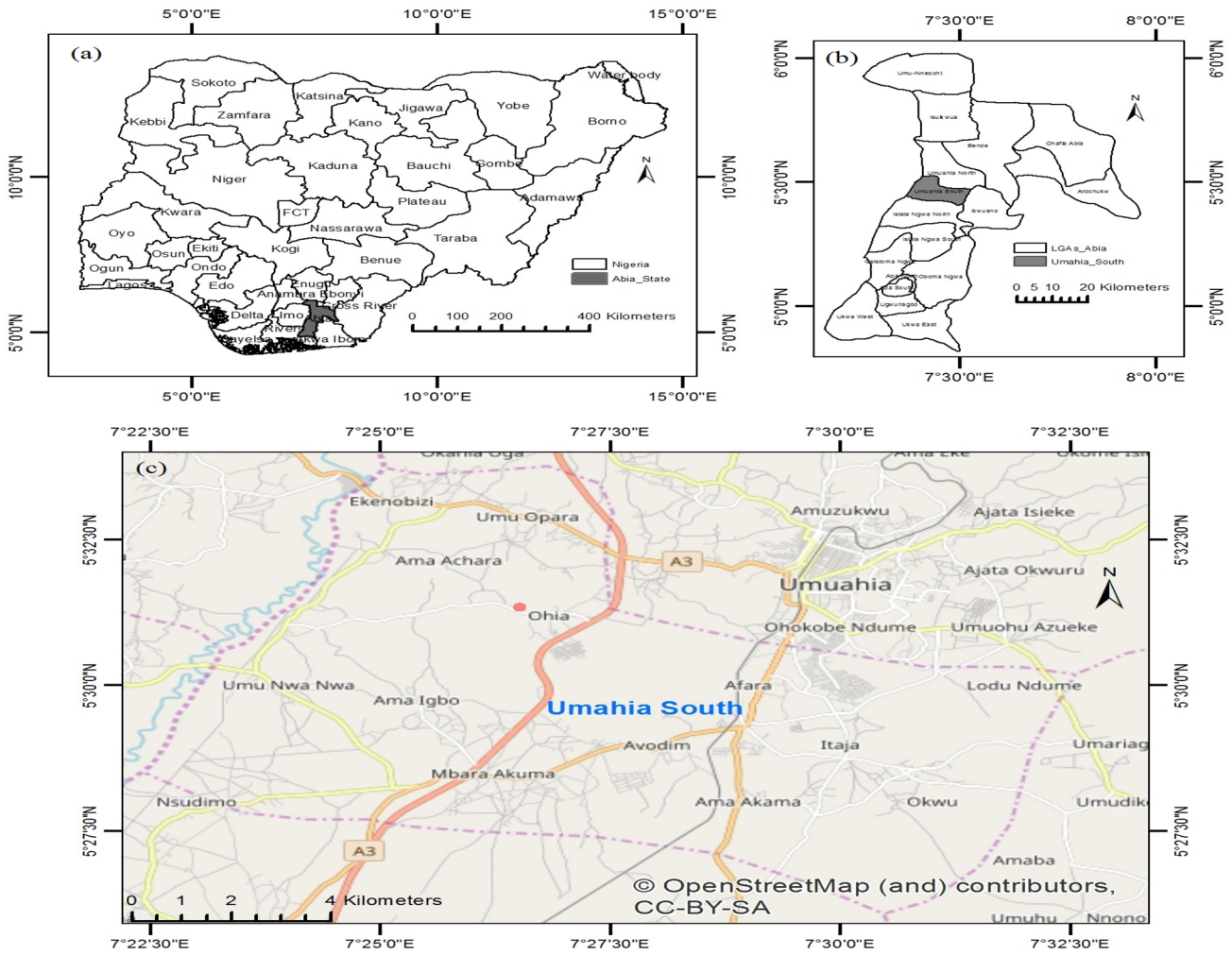


Fig. 2 Location map of borrow pit

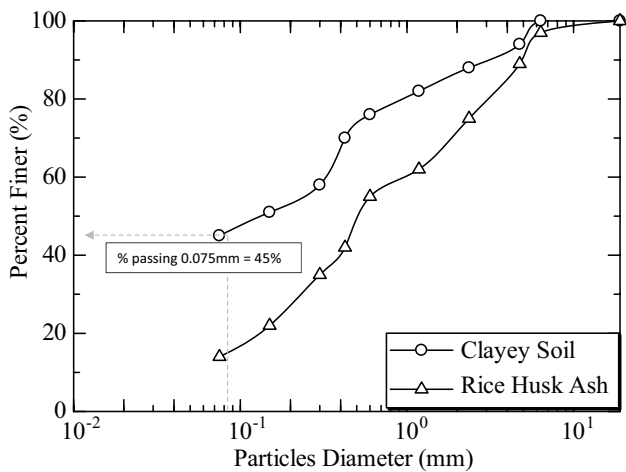


Fig. 3 Particle size distribution curve of clayey soil and rice husk ash [17]

limit (%), plasticity index (%) and compression index estimated using Skempton’s compression index–liquid limit relationship [29]. Furthermore, the generated datasets (see “Appendix 1”) were deployed in the intelligent prediction exercise employing genetic programming (GP) technique.

In this research, 121 data records include C_c^s and the corresponding tests’ results of hybrid cement ratio (Hc), nanostructured quarry fines ratio (NQF), coefficient of curvature (Cc), coefficient of uniformity (Cu), maximum dry density (δ_{max}), optimum moisture content (w_{max}), partial maximum dry density (δ_{part}), liquid limit (w_L) and plasticity index (Ip).

For each record, the C_c^s values were calculated using Skempton’s formula ($C_c^s = 0.007(w_L - 10)$). Accordingly, the liquid limit (w_L) values are excluded from the inputs of the database; also to keep all inputs dimensionless, a factor $\frac{\sigma_{part}}{\sigma_{max}}$ known as the degree of compaction is used instead of the two individual factors (δ_{max}) and (δ_{part}). The

Fig. 4 Morphology of silica-rich RHA [17]

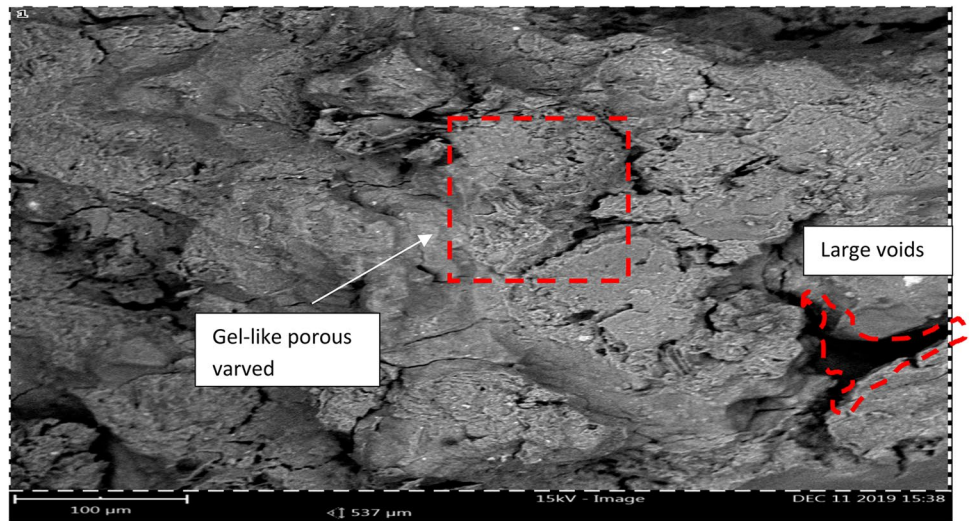


Fig. 5 Morphology of expansive soil [17]

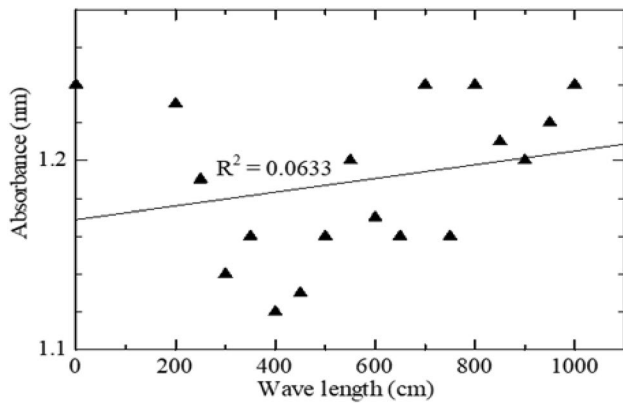
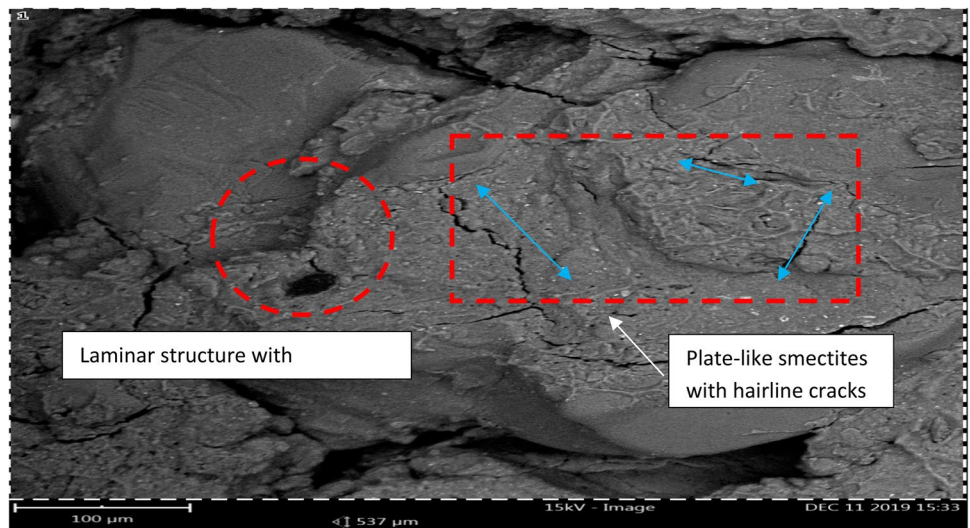


Fig. 6 UV-Vis spectrophotometric nanograph of nanostructured quarry fines

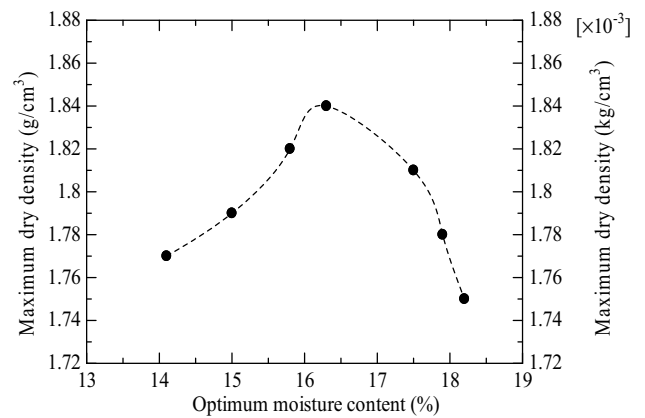


Fig. 7 Compaction characteristics of lateritic soil sample

considered inputs and the characteristics of each (GP) trial are summarized and presented.

The collected records were divided into two sets. The first one is a training set that contains 80 records, while the second one is the validation set that contains 41 records. The complete dataset is shown in “Appendix 2”. Statistical analysis for the utilized database is summarized and presented to show the significant variability in the soil properties.

Results and Discussion

Preliminary characterization and stabilization geotechnics

Table 1 shows the pozzolanic content of the materials utilized in this soil treatment experiment derived through XRF exposure. This shows that the HC has the highest aluminosilicate composition of 88.73 compared to NQF with 87.74% and RHA with 82.97% corresponding to total of Al₂O₃, SiO₂ and Fe₂O₃ compositions and these meet the materials standard for supplementary cementitious materials (SCMs) proposed by ASTM C618 [4]. From the foregoing requirements, it can be observed that HC is an improved composite of RHA with higher capacity to cement materials. The effect of these multiple binders HC and NQF on the grading factors (C_c and C_u), maximum dry densities, moisture and consistency parameters, and compression index is presented

in Figs. 8, 9, 10 and 11, respectively. It can be observed that the increased varying proportion of the multiple binders consistently improved the studied treated soil parameters. This behaviour shows the binding effect due to hydration, pozzolanic reaction, cation exchange and densification of the treated soil with increased binders. This also may be due to the increased nucleating and reactive surface achieved through nanotexturing the quarry dust through complete pulverization and nano-sieving. This linear consistency in parameters substantial improvement has a huge influence on the proposed models’ performance.

Genetic programming prediction of compression index

Statistical analysis of database

Table 2 shows the statistical descriptions of the independent and dependent variables being considered in this evolutionary prediction models. This shows minimum and maximum ranges for all independent and dependent variables. The standard deviation (SD) and variance (Var) are also presented for each variable in agreement with the findings of Edjabou et al. [10]. From this finding, it shows that the smaller the value of SD, the closer most of the values are to the average of the variables (HC, NQF, C_c, C_u, W_{max}, I_p, degree of compaction and C_c^s), whereas a larger SD implies that the range of outcomes

Table 1 Chemical oxide composition of the additive materials

| Materials | Oxides’ composition (content by weight, %) | | | | | | | | | | | | |
|---------------|--|--------------------------------|------|--------------------------------|------|------------------|-------------------|------------------|------|-------------------------------|-----------------|----|----------|
| | SiO ₂ | Al ₂ O ₃ | CaO | Fe ₂ O ₃ | MgO | K ₂ O | Na ₂ O | TiO ₂ | LOI | P ₂ O ₅ | SO ₃ | IR | Free CaO |
| Clay soil | 12.45 | 18.09 | 2.30 | 10.66 | 4.89 | 12.10 | 34.33 | 0.07 | – | 5.11 | – | – | – |
| Rice husk ash | 56.48 | 22.72 | 5.56 | 3.77 | 4.65 | 2.76 | 0.01 | 3.17 | 0.88 | – | – | – | – |
| HC | 59.12 | 25.3 | 6.3 | 4.23 | 2.5 | 1.21 | – | 1.34 | – | – | – | – | – |
| NQF | 62.48 | 18.72 | 4.83 | 6.54 | 2.56 | 3.18 | – | 0.29 | 1.01 | – | – | – | – |

*IR is insoluble residue; LOI is loss on ignition

Fig. 8 Coefficients of uniformity and curvature of treated soil response with multiple-binder addition

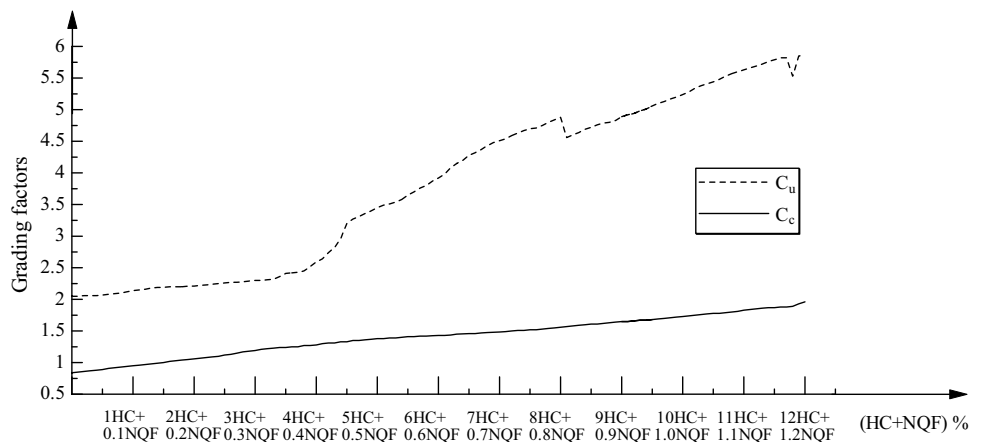


Fig. 9 Maximum dry densities of treated soil responses with multiple-binder addition

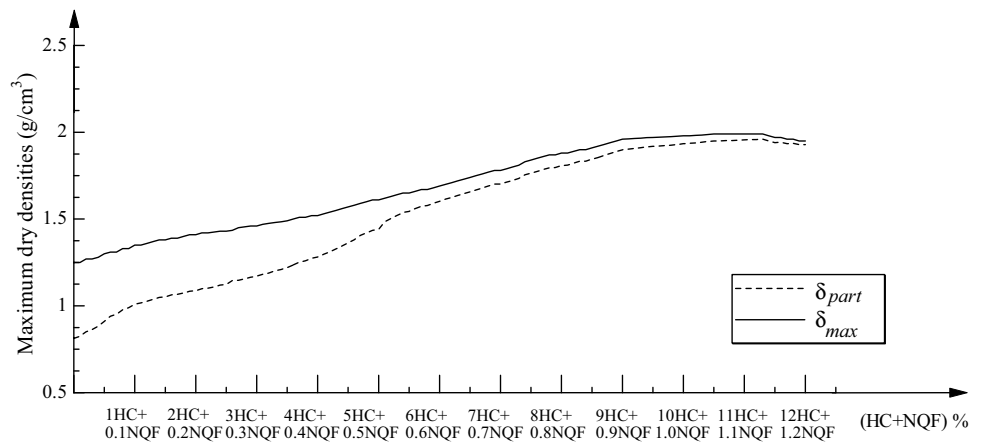


Fig. 10 Liquid limit, plasticity index and optimum moisture content of treated soil responses with multiple-binder addition

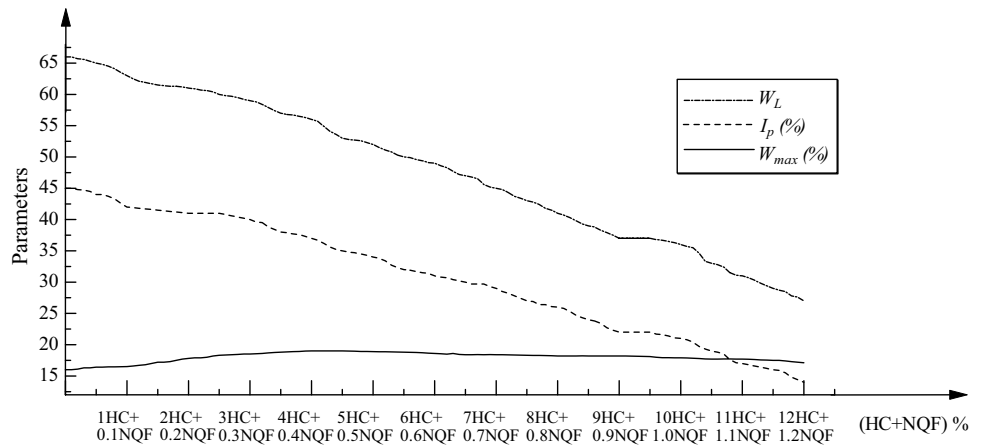
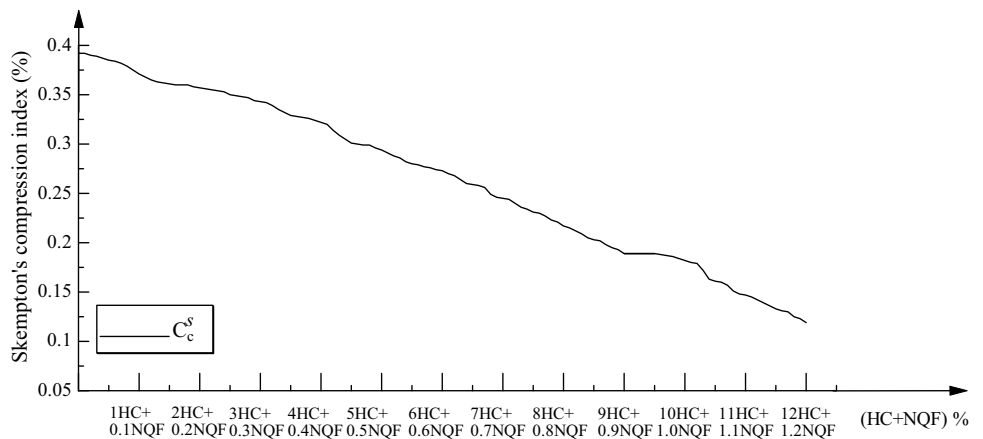


Fig. 11 Compression index of treated soil response with multiple-binder addition



are more outspread. Variance quantifies the asymmetry of the probability distribution of real-valued random variables with respect to its average (mean). According to Sharma and Ojha [27], it can be positive, zero, negative or out of number line.

Research program

Four trials have been considered in this model prediction procedure to correlate the measured values of C_c^s to the matching experimental tests measurements. Each

prediction trial makes use of a particular level of complexity starting from two-level expression and up to five-level expression. Iterations are conducted until the minimum (SSR) of the set which reflects the most accurate expression at the considered level of complexity is achieved. Characteristics of each trial are summarized in Table 3.

The following paragraphs present and discuss the results of each trial. Results of all trials are summarized in Table 4. Included in all the conducted trials, the main target was to make a comparison between

the GP compression index predicted models C_C^{GP} and the measured C_C^s values and hence evaluate the accuracy of the developed expressions based on statistical analysis.

Prediction of C_C^{GP} value using (GP) and performance evaluation of models

Trial No. (1) In this trial, a simple expression with only two levels of complexity was considered and analysed. Equation (4) shows the best fitting expression with the minimum

Table 2 Statistical analysis of collected database

| | HC | NQF | Cc | Cu | W_{max} | I_p | $\frac{\sigma_{part}}{\sigma_{max}}$ | C_C^s |
|-----------------------|------|------|------|------|-----------|-------|--------------------------------------|---------|
| <i>Training set</i> | | | | | | | | |
| Max | 0.12 | 0.01 | 1.96 | 5.86 | 0.19 | 0.45 | 0.99 | 0.39 |
| Min | 0.00 | 0.00 | 0.84 | 2.05 | 0.16 | 0.14 | 0.65 | 0.12 |
| Avg | 0.06 | 0.01 | 1.39 | 3.76 | 0.18 | 0.31 | 0.88 | 0.27 |
| SD | 0.04 | 0.00 | 0.32 | 1.37 | 0.01 | 0.10 | 0.11 | 0.09 |
| Var | 0.64 | 0.64 | 0.23 | 0.36 | 0.05 | 0.31 | 0.12 | 0.32 |
| <i>Validation set</i> | | | | | | | | |
| Max | 0.12 | 0.01 | 1.93 | 5.85 | 0.19 | 0.42 | 0.99 | 0.37 |
| Min | 0.01 | 0.00 | 0.95 | 2.14 | 0.17 | 0.14 | 0.75 | 0.12 |
| Avg | 0.06 | 0.01 | 1.45 | 3.87 | 0.18 | 0.30 | 0.91 | 0.26 |
| SD | 0.03 | 0.00 | 0.23 | 1.20 | 0.01 | 0.08 | 0.08 | 0.07 |
| Var | 0.46 | 0.46 | 0.16 | 0.31 | 0.03 | 0.26 | 0.08 | 0.27 |

Table 3 Characteristics of each (GP) trial

| Trial No. | No. of levels | Used variables | Population size | Survivors size | No. of generations | Mutation present |
|-----------|---------------|---|-----------------|----------------|--------------------|------------------|
| 1 | 2 | (HC), (NQF), (Cc), (Cu), (w_{max}), ($\gamma_{part}/\gamma_{max}$), (I_p); (1, 3, 5, 7, 11) | 10,000 | 3000 | 50 | 5% |
| 2 | 3 | | 25,000 | 7500 | 75 | |
| 3 | 4 | | 50,000 | 15,000 | 100 | |
| 4 | 5 | | 100,000 | 30,000 | 150 | |

Table 4 Summary for the accuracy of (GP) formulas from all trails

| Trial No. | No. of levels | Proposed formula | Error % | | | R^2 | | |
|-----------|---------------|------------------|----------|------------|--------|----------|------------|--------|
| | | | Training | Validation | Total | Training | Validation | Total |
| 1 | 2 | Equation (4) | 0.0052 | 0.0043 | 0.0048 | 0.9991 | 0.9981 | 0.9988 |
| 2 | 3 | Equation (5) | 0.0029 | 0.0036 | 0.0031 | 0.9991 | 0.9982 | 0.9989 |
| 3 | 4 | Equation (6) | 0.0029 | 0.0035 | 0.0031 | 0.9991 | 0.9982 | 0.9989 |
| 4 | 5 | Equation (7) | 0.0027 | 0.0035 | 0.0030 | 0.9991 | 0.9982 | 0.9989 |

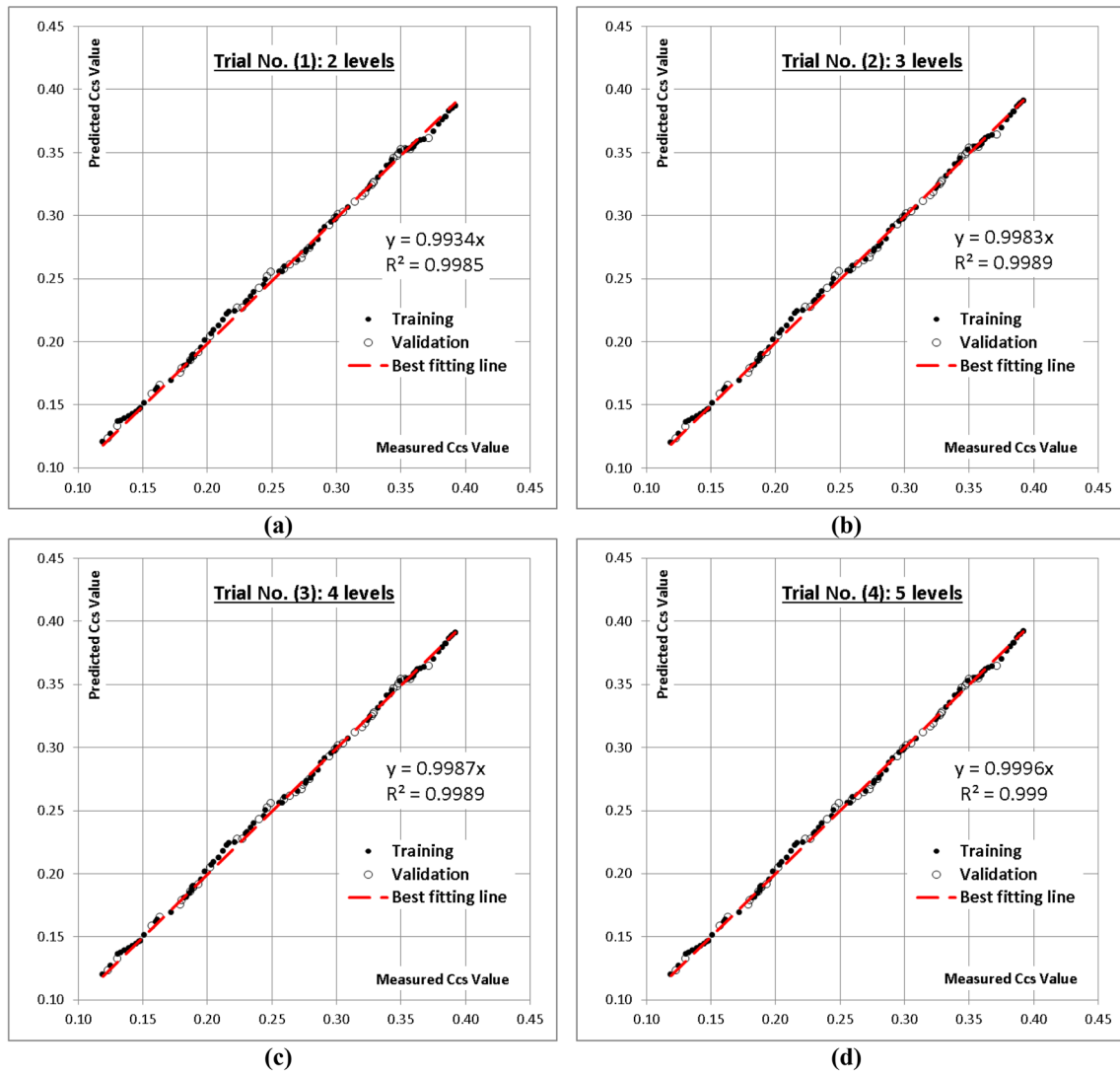


Fig. 12 Relation between the predicted and measured C_C^s values using the different developed correlations

SSR error through this trial. Figure 12(a) represents the correlation between measured and predicted C_C^{GP} values using Eq. (4)

$$C_C^{GP} = 0.86I_p. \tag{4}$$

According to the performed statistical analysis, the achieved error values for training set, validation set and total set are (0.0052%), (0.0043%) and (0.0048%), respectively, with corresponding coefficient of determination (R^2) values of (0.9991), (0.9981) and (0.9988). The archived (R^2) values indicate an excellent correlation

between the predicted and experimental C_C^{GP} values. Equation 4 also shows that the plasticity index I_p has the greatest influence on the compression index behaviour of the treated unsaturated soil.

Trial No. (2) In this trial, the complexity level is increased to three levels. Equation (5) shows the best achieved correlation, while Fig. 12(b) provides the comparison between the predicted and experimental C_C^{GP} values. Error values for the training set, validation set and total set achieved using this equation are (0.0029%), (0.0036%) and (0.0031%), respectively. The corresponding (R^2) values

are (0.9991), (0.9982) and (0.9989). Comparing between the (R^2) values of Eqs. 4 and 5 shows that Eq. (5) is more accurate than Eq. (4).

$$C_C^{GP} = \frac{(I_p - Hc \cdot NQF)}{\ln(w_{\max} + 3.0)} \quad (5)$$

Trial No. (3) In this case, four levels of complexity were considered to produce the best achieved expression as given in Eq. (6). The correlation between the predicted and experimental C_C^{GP} values is shown in Fig. 12(c). For this case, the achieved error values for the training set, validation set and total set are (0.0029%), (0.0035%) and (0.0031%), respectively, while the corresponding (R^2) values are (0.9991), (0.9982) and (0.9989). Comparing the accuracies of Eqs. (5) and (6) shows almost no improvement in the accuracy.

$$C_C^{GP} = \frac{(I_p - Hc \cdot NQF) (\sigma_{part} / \sigma_{\max})^{NQF}}{\ln(w_{\max} + 3.0)}. \quad (6)$$

Trial No. (4) In order to investigate the effect of using five levels of complexity, another trial was performed. The best produced expression was as given by Eq. (7). The correlation between the experimental and predicted C_C^{GP} values using this equation is shown in Fig. 12(d). Achieved error values for the training set, validation set and total set are (0.0027%), (0.0035%) and (0.0030%), respectively, while the corresponding (R^2) values are (0.9991), (0.9982) and (0.9989). The accuracy of this case is almost comparable to the correlation given in the second trial and expressed by Eq. (5).

$$C_C^{GP} = \frac{(I_p - Hc \cdot NQF) \left[(\sigma_{part} / \sigma_{\max})^{NQF} \right]^{(I_p / w_{\max})}}{\ln(w_{\max} + 3.0)}. \quad (7)$$

Conclusions

Genetic programming approach has been used to predict models for the compression index of unsaturated soil treated with bi-mixed binders, hybrid cement (HC), made by activating rice husk ash (RHA) with hydrated lime and nanostructured quarry fines (NQF) made from pulverized and 200-nm sieved quarry dust (QD). From the foregoing, the following can be remarked:

- Unsaturated soil with a saturation degree of 60 was basically classified as highly plastic A-7-6 group of soil and unsuitable for use as a foundation material especially under hydraulically bound environments.
- The geotechnics behaviour of the treated soil showed substantial and consistent improvement on the studied parameters with the addition of HC and NQF, which shows the binding efficiency of the clean and green binders with zero carbon footprint.
- Several parameters of the treated soil were studied and deployed as the independent variables after generating multiple datasets.
- The GP adopted four-trial methods to propose four models as functions of the influence of the studied parameters.
- The performance of the models was evaluated, and it was observed that the second, third and fourth trials presented the better trials with a coefficient of determination of 0.9989 than the first trial with a coefficient of determination of 0.9988.
- However, the error analysis showed that the fourth trial has the least error of 0.003.
- Generally, GP has shown its flexibility in the prediction of multiple models of a geotechnics problem with high-performance indices.

Table 5 Treated and untreated soil (degree of saturation, Sr of 60%) with nine input parameters, one output parameter and 121 datasets

| Input properties of treated and untreated soil | | | | | | | | | | Output |
|--|---------|-------|-------|-----------------------------------|--------------|--|---------|---------|-----------|--------|
| HC (%) | NQF (%) | C_C | C_u | δ_{\max} g/cm ³ | w_{\max} % | δ_{part} g/cm ³ | w_L % | I_P % | C_C^s % | |
| 0 | 0 | 0.84 | 2.05 | 1.25 | 16 | 0.8125 | 66 | 45 | 0.392 | |
| 0.1 | 0.01 | 0.85 | 2.05 | 1.25 | 16 | 0.825 | 66 | 45 | 0.392 | |
| 0.2 | 0.02 | 0.86 | 2.06 | 1.27 | 16.1 | 0.8509 | 65.7 | 44.8 | 0.390 | |
| 0.3 | 0.03 | 0.87 | 2.06 | 1.27 | 16.3 | 0.8636 | 65.6 | 44.7 | 0.389 | |
| 0.4 | 0.04 | 0.88 | 2.06 | 1.28 | 16.3 | 0.8832 | 65.3 | 44.5 | 0.387 | |
| 0.5 | 0.05 | 0.89 | 2.07 | 1.30 | 16.4 | 0.91 | 65 | 44 | 0.385 | |
| 0.6 | 0.06 | 0.91 | 2.08 | 1.31 | 16.4 | 0.94058 | 64.8 | 44 | 0.384 | |
| 0.7 | 0.07 | 0.92 | 2.09 | 1.31 | 16.45 | 0.95106 | 64.5 | 43.7 | 0.382 | |
| 0.8 | 0.08 | 0.93 | 2.1 | 1.33 | 16.47 | 0.97755 | 64.1 | 43.3 | 0.379 | |
| 0.9 | 0.09 | 0.94 | 2.12 | 1.33 | 16.49 | 0.98952 | 63.5 | 42.6 | 0.375 | |
| 1 | 0.1 | 0.95 | 2.14 | 1.35 | 16.5 | 1.0098 | 63 | 42 | 0.371 | |
| 1.1 | 0.11 | 0.96 | 2.15 | 1.35 | 16.6 | 1.01655 | 62.5 | 41.9 | 0.368 | |
| 1.2 | 0.12 | 0.97 | 2.16 | 1.36 | 16.7 | 1.0268 | 62.1 | 41.8 | 0.365 | |
| 1.3 | 0.13 | 0.98 | 2.18 | 1.37 | 16.8 | 1.03709 | 61.9 | 41.7 | 0.363 | |
| 1.4 | 0.14 | 0.99 | 2.19 | 1.38 | 17 | 1.0488 | 61.7 | 41.6 | 0.362 | |
| 1.5 | 0.15 | 1 | 2.19 | 1.38 | 17.2 | 1.05156 | 61.5 | 41.5 | 0.361 | |
| 1.6 | 0.16 | 1.02 | 2.2 | 1.39 | 17.2 | 1.06335 | 61.4 | 41.4 | 0.360 | |
| 1.7 | 0.17 | 1.03 | 2.2 | 1.39 | 17.3 | 1.06613 | 61.3 | 41.3 | 0.360 | |
| 1.8 | 0.18 | 1.04 | 2.2 | 1.4 | 17.5 | 1.0738 | 61.3 | 41.2 | 0.360 | |
| 1.9 | 0.19 | 1.05 | 2.21 | 1.41 | 17.7 | 1.08429 | 61.2 | 41.1 | 0.358 | |
| 2 | 0.2 | 1.06 | 2.21 | 1.41 | 17.8 | 1.08711 | 61 | 41 | 0.357 | |
| 2.1 | 0.21 | 1.07 | 2.22 | 1.42 | 17.9 | 1.09908 | 60.9 | 41 | 0.356 | |
| 2.2 | 0.22 | 1.08 | 2.23 | 1.42 | 17.9 | 1.10192 | 60.7 | 41 | 0.355 | |
| 2.3 | 0.23 | 1.09 | 2.24 | 1.425 | 18 | 1.10865 | 60.6 | 41 | 0.354 | |
| 2.4 | 0.24 | 1.1 | 2.25 | 1.43 | 18.2 | 1.11969 | 60.4 | 41 | 0.353 | |
| 2.5 | 0.25 | 1.12 | 2.26 | 1.43 | 18.3 | 1.12255 | 60 | 41 | 0.350 | |
| 2.6 | 0.26 | 1.13 | 2.27 | 1.435 | 18.35 | 14.4598 | 59.8 | 40.8 | 0.349 | |
| 2.7 | 0.27 | 1.15 | 2.27 | 1.45 | 18.4 | 1.14695 | 59.7 | 40.6 | 0.348 | |
| 2.8 | 0.28 | 1.17 | 2.28 | 1.455 | 18.45 | 1.15527 | 59.5 | 40.4 | 0.347 | |
| 2.9 | 0.29 | 1.18 | 2.29 | 1.46 | 18.5 | 1.16508 | 59.2 | 40.2 | 0.344 | |
| 3 | 0.3 | 1.19 | 2.3 | 1.46 | 18.5 | 1.17092 | 59 | 40 | 0.343 | |
| 3.1 | 0.31 | 1.21 | 2.3 | 1.47 | 18.55 | 1.18188 | 58.8 | 39.6 | 0.342 | |
| 3.2 | 0.32 | 1.22 | 2.31 | 1.475 | 18.6 | 1.18885 | 58.4 | 39.5 | 0.339 | |
| 3.3 | 0.33 | 1.23 | 2.32 | 1.48 | 18.7 | 1.20176 | 57.9 | 38.8 | 0.335 | |
| 3.4 | 0.34 | 1.24 | 2.36 | 1.484 | 18.75 | 1.20946 | 57.4 | 38.4 | 0.332 | |
| 3.5 | 0.35 | 1.24 | 2.41 | 1.49 | 18.8 | 1.22031 | 57 | 38 | 0.329 | |
| 3.6 | 0.36 | 1.25 | 2.42 | 1.5 | 18.85 | 1.236 | 56.8 | 37.9 | 0.328 | |
| 3.7 | 0.37 | 1.25 | 2.43 | 1.51 | 18.9 | 1.25179 | 56.7 | 37.7 | 0.327 | |
| 3.8 | 0.38 | 1.27 | 2.45 | 1.51 | 18.93 | 1.25934 | 56.5 | 37.6 | 0.326 | |
| 3.9 | 0.39 | 1.27 | 2.52 | 1.52 | 18.98 | 1.27376 | 56.3 | 37.3 | 0.324 | |
| 4 | 0.4 | 1.28 | 2.59 | 1.52 | 19.0 | 1.28136 | 56 | 37 | 0.322 | |
| 4.1 | 0.41 | 1.30 | 2.64 | 1.53 | 19.0 | 1.29744 | 55.7 | 36.7 | 0.320 | |
| 4.2 | 0.42 | 1.31 | 2.74 | 1.54 | 19.0 | 1.31054 | 54.9 | 36.2 | 0.314 | |
| 4.3 | 0.43 | 1.31 | 2.82 | 1.55 | 19.0 | 1.32835 | 54.1 | 35.6 | 0.309 | |
| 4.4 | 0.44 | 1.33 | 2.96 | 1.56 | 19.0 | 1.34472 | 53.6 | 35.2 | 0.305 | |
| 4.5 | 0.45 | 1.33 | 3.2 | 1.57 | 19.0 | 1.36276 | 53 | 35 | 0.301 | |
| 4.6 | 0.46 | 1.35 | 3.27 | 1.58 | 18.98 | 1.38092 | 52.8 | 34.8 | 0.300 | |
| 4.7 | 0.47 | 1.35 | 3.31 | 1.59 | 18.96 | 1.40556 | 52.7 | 34.7 | 0.299 | |
| 4.8 | 0.48 | 1.36 | 3.36 | 1.60 | 18.93 | 1.4208 | 52.6 | 34.5 | 0.299 | |

Table 5 (continued)

| Input properties of treated and untreated soil | | | | | | | | | Output |
|--|---------|-------|-------|-----------------------------------|--------------|--|---------|---------|-----------|
| HC (%) | NQF (%) | C_C | C_u | δ_{\max} g/cm ³ | w_{\max} % | δ_{part} g/cm ³ | w_L % | I_P % | C_C^S % |
| 4.9 | 0.49 | 1.37 | 3.4 | 1.61 | 18.91 | 1.43451 | 52.3 | 34.3 | 0.296 |
| 5 | 0.5 | 1.38 | 3.45 | 1.61 | 18.9 | 1.44095 | 52 | 34 | 0.294 |
| 5.1 | 0.51 | 1.38 | 3.49 | 1.62 | 18.88 | 1.48392 | 51.5 | 33.8 | 0.291 |
| 5.2 | 0.52 | 1.39 | 3.51 | 1.63 | 18.86 | 1.50286 | 51.1 | 33.4 | 0.288 |
| 5.3 | 0.53 | 1.39 | 3.54 | 1.64 | 18.84 | 1.52028 | 50.8 | 32.7 | 0.286 |
| 5.4 | 0.54 | 1.4 | 3.58 | 1.65 | 18.82 | 1.5378 | 50.3 | 32.3 | 0.282 |
| 5.5 | 0.55 | 1.41 | 3.65 | 1.65 | 18.8 | 1.5444 | 50 | 32 | 0.28 |
| 5.6 | 0.56 | 1.41 | 3.7 | 1.66 | 18.78 | 1.5604 | 49.9 | 31.9 | 0.279 |
| 5.7 | 0.57 | 1.42 | 3.76 | 1.67 | 18.75 | 1.57314 | 49.6 | 31.7 | 0.277 |
| 5.8 | 0.58 | 1.42 | 3.8 | 1.67 | 18.71 | 1.57815 | 49.4 | 31.5 | 0.276 |
| 5.9 | 0.59 | 1.425 | 3.87 | 1.68 | 18.65 | 1.59096 | 49.1 | 31.4 | 0.274 |
| 6 | 0.6 | 1.43 | 3.92 | 1.69 | 18.6 | 1.60212 | 49 | 31 | 0.273 |
| 6.1 | 0.61 | 1.43 | 3.98 | 1.7 | 18.55 | 1.615 | 48.6 | 30.8 | 0.270 |
| 6.2 | 0.62 | 1.435 | 4.08 | 1.71 | 18.48 | 1.6245 | 48.3 | 30.7 | 0.268 |
| 6.3 | 0.63 | 1.45 | 4.15 | 1.72 | 18.6 | 1.63572 | 47.7 | 30.4 | 0.264 |
| 6.4 | 0.64 | 1.455 | 4.2 | 1.73 | 18.44 | 1.64696 | 47.2 | 30.2 | 0.260 |
| 6.5 | 0.65 | 1.46 | 4.28 | 1.74 | 18.4 | 1.65648 | 47 | 30 | 0.259 |
| 6.6 | 0.66 | 1.46 | 4.32 | 1.75 | 18.4 | 1.66775 | 46.8 | 29.7 | 0.258 |
| 6.7 | 0.67 | 1.47 | 4.37 | 1.76 | 18.41 | 1.67904 | 46.5 | 29.7 | 0.256 |
| 6.8 | 0.68 | 1.475 | 4.43 | 1.77 | 18.4 | 1.69035 | 45.6 | 29.7 | 0.249 |
| 6.9 | 0.69 | 1.48 | 4.48 | 1.78 | 18.41 | 1.70168 | 45.2 | 29.3 | 0.246 |
| 7 | 0.7 | 1.484 | 4.51 | 1.78 | 18.4 | 1.70168 | 45 | 29 | 0.245 |
| 7.1 | 0.71 | 1.49 | 4.54 | 1.79 | 18.39 | 1.71303 | 44.8 | 28.5 | 0.244 |
| 7.2 | 0.72 | 1.5 | 4.59 | 1.8 | 18.37 | 1.7226 | 44.3 | 28.2 | 0.240 |
| 7.3 | 0.73 | 1.51 | 4.63 | 1.81 | 18.35 | 1.73398 | 43.7 | 27.8 | 0.236 |
| 7.4 | 0.74 | 1.51 | 4.67 | 1.83 | 18.32 | 1.75497 | 43.4 | 27.4 | 0.234 |
| 7.5 | 0.75 | 1.52 | 4.7 | 1.84 | 18.3 | 1.76456 | 43 | 27 | 0.231 |
| 7.6 | 0.76 | 1.52 | 4.71 | 1.85 | 18.29 | 1.77415 | 42.8 | 26.9 | 0.230 |
| 7.7 | 0.77 | 1.53 | 4.75 | 1.86 | 18.28 | 1.7856 | 42.4 | 26.4 | 0.227 |
| 7.8 | 0.78 | 1.54 | 4.8 | 1.87 | 18.26 | 1.7952 | 41.8 | 26.4 | 0.223 |
| 7.9 | 0.79 | 1.55 | 4.84 | 1.87 | 18.23 | 1.79707 | 41.5 | 26.1 | 0.221 |
| 8 | 0.8 | 1.56 | 4.88 | 1.88 | 18.2 | 1.80856 | 41 | 26 | 0.217 |
| 8.1 | 0.81 | 1.57 | 4.56 | 1.88 | 18.2 | 1.81044 | 40.7 | 25.8 | 0.215 |
| 8.2 | 0.82 | 1.58 | 4.6 | 1.89 | 18.2 | 1.82196 | 40.3 | 25.3 | 0.212 |
| 8.3 | 0.83 | 1.59 | 4.64 | 1.90 | 18.2 | 1.8335 | 39.8 | 24.7 | 0.209 |
| 8.4 | 0.84 | 1.60 | 4.69 | 1.90 | 18.21 | 1.8335 | 39.3 | 24.3 | 0.205 |
| 8.5 | 0.85 | 1.61 | 4.72 | 1.91 | 18.2 | 1.84506 | 39 | 24 | 0.203 |
| 8.6 | 0.86 | 1.61 | 4.76 | 1.92 | 18.2 | 1.85472 | 38.8 | 23.8 | 0.202 |
| 8.7 | 0.87 | 1.62 | 4.79 | 1.93 | 18.2 | 1.86631 | 38.3 | 23.4 | 0.198 |
| 8.8 | 0.88 | 1.63 | 4.8 | 1.94 | 18.2 | 1.87792 | 37.9 | 22.7 | 0.195 |
| 8.9 | 0.89 | 1.64 | 4.83 | 1.95 | 18.2 | 1.88955 | 37.5 | 22.3 | 0.193 |
| 9 | 0.9 | 1.65 | 4.89 | 1.96 | 18.2 | 1.89924 | 37 | 22 | 0.189 |
| 9.1 | 0.91 | 1.65 | 4.92 | 1.962 | 18.19 | 1.90314 | 37 | 22 | 0.189 |
| 9.2 | 0.92 | 1.66 | 4.94 | 1.964 | 18.18 | 1.907044 | 37 | 22 | 0.189 |
| 9.3 | 0.93 | 1.67 | 4.98 | 1.966 | 18.16 | 1.910952 | 37 | 22 | 0.189 |
| 9.4 | 0.94 | 1.67 | 5.01 | 1.969 | 18.13 | 1.915837 | 37 | 22 | 0.189 |
| 9.5 | 0.95 | 1.68 | 5.06 | 1.97 | 18.1 | 1.91878 | 37 | 22 | 0.189 |
| 9.6 | 0.96 | 1.69 | 5.1 | 1.972 | 18 | 1.920728 | 36.8 | 21.7 | 0.188 |
| 9.7 | 0.97 | 1.7 | 5.13 | 1.973 | 17.92 | 1.923675 | 36.7 | 21.6 | 0.187 |

Table 5 (continued)

| Input properties of treated and untreated soil | | | | | | | | | | Output |
|--|---------|-------|-------|-----------------------------------|--------------|--|---------|---------|-----------|--------|
| HC (%) | NQF (%) | C_C | C_u | δ_{\max} g/cm ³ | w_{\max} % | δ_{part} g/cm ³ | w_L % | I_P % | C_C^s % | |
| 9.8 | 0.98 | 1.71 | 5.17 | 1.975 | 17.93 | 1.925625 | 36.5 | 21.4 | 0.186 | |
| 9.9 | 0.99 | 1.72 | 5.2 | 1.977 | 17.91 | 1.929552 | 36.3 | 21.1 | 0.184 | |
| 10 | 1 | 1.73 | 5.24 | 1.98 | 17.9 | 1.93446 | 36 | 21 | 0.182 | |
| 10.1 | 1.01 | 1.74 | 5.28 | 1.98 | 17.88 | 1.93644 | 35.7 | 20.8 | 0.180 | |
| 10.2 | 1.02 | 1.75 | 5.34 | 1.982 | 17.84 | 1.938396 | 35.5 | 20.4 | 0.179 | |
| 10.3 | 1.03 | 1.76 | 5.38 | 1.984 | 17.79 | 1.942336 | 34.6 | 19.7 | 0.172 | |
| 10.4 | 1.04 | 1.77 | 5.41 | 1.987 | 17.73 | 1.94726 | 33.3 | 19.3 | 0.163 | |
| 10.5 | 1.05 | 1.78 | 5.44 | 1.99 | 17.7 | 1.9502 | 33 | 19 | 0.161 | |
| 10.6 | 1.06 | 1.78 | 5.48 | 1.99 | 17.7 | 1.9502 | 32.8 | 18.8 | 0.160 | |
| 10.7 | 1.07 | 1.79 | 5.53 | 1.99 | 17.71 | 1.95219 | 32.4 | 18.5 | 0.157 | |
| 10.8 | 1.08 | 1.8 | 5.57 | 1.99 | 17.71 | 1.95219 | 31.5 | 17.6 | 0.151 | |
| 10.9 | 1.09 | 1.81 | 5.6 | 1.99 | 17.7 | 1.95418 | 31.1 | 17.1 | 0.148 | |
| 11 | 1.1 | 1.83 | 5.63 | 1.99 | 17.7 | 1.95617 | 31 | 17 | 0.147 | |
| 11.1 | 1.11 | 1.84 | 5.66 | 1.99 | 17.68 | 1.95816 | 30.7 | 16.8 | 0.145 | |
| 11.2 | 1.12 | 1.85 | 5.69 | 1.99 | 17.63 | 1.95816 | 30.3 | 16.6 | 0.142 | |
| 11.3 | 1.13 | 1.86 | 5.72 | 1.99 | 17.57 | 1.96015 | 29.8 | 16.4 | 0.139 | |
| 11.4 | 1.14 | 1.87 | 5.76 | 1.98 | 17.53 | 1.9503 | 29.4 | 16.2 | 0.136 | |
| 11.5 | 1.15 | 1.87 | 5.79 | 1.97 | 17.5 | 1.94045 | 29 | 16 | 0.133 | |
| 11.6 | 1.16 | 1.88 | 5.82 | 1.97 | 17.5 | 1.94242 | 28.7 | 15.9 | 0.131 | |
| 11.7 | 1.17 | 1.88 | 5.82 | 1.96 | 17.4 | 1.93452 | 28.5 | 15.5 | 0.130 | |
| 11.8 | 1.18 | 1.89 | 5.53 | 1.96 | 17.3 | 1.93648 | 27.8 | 14.8 | 0.125 | |
| 11.9 | 1.19 | 1.93 | 5.85 | 1.95 | 17.2 | 1.92855 | 27.6 | 14.4 | 0.123 | |
| 12 | 1.2 | 1.96 | 5.86 | 1.95 | 17.1 | 1.92855 | 27 | 14 | 0.119 | |

Appendix 1

See Table 5.

Table 6 Treated and untreated soil (degree of saturation, Sr of 60%) with seven input parameters, one output parameter and 121 datasets

| # | HC | NQF | Cc | Cu | w _{max} | Ip | $\sigma_{\text{part}}/\sigma_{\text{max}}$ | Ccs |
|---------------------|-------|-------|------|------|------------------|------|--|-------|
| <i>Training set</i> | | | | | | | | |
| 1 | 0.016 | 0.002 | 1.02 | 2.20 | 0.17 | 0.41 | 0.77 | 0.360 |
| 2 | 0.120 | 0.012 | 1.96 | 5.86 | 0.17 | 0.14 | 0.99 | 0.119 |
| 3 | 0.067 | 0.007 | 1.47 | 4.37 | 0.18 | 0.30 | 0.95 | 0.256 |
| 4 | 0.043 | 0.004 | 1.31 | 2.82 | 0.19 | 0.36 | 0.86 | 0.309 |
| 5 | 0.070 | 0.007 | 1.48 | 4.51 | 0.18 | 0.29 | 0.96 | 0.245 |
| 6 | 0.003 | 0.000 | 0.87 | 2.06 | 0.16 | 0.45 | 0.68 | 0.389 |
| 7 | 0.030 | 0.003 | 1.19 | 2.30 | 0.19 | 0.40 | 0.80 | 0.343 |
| 8 | 0.015 | 0.002 | 1.00 | 2.19 | 0.17 | 0.42 | 0.76 | 0.361 |
| 9 | 0.011 | 0.001 | 0.96 | 2.15 | 0.17 | 0.42 | 0.75 | 0.368 |
| 10 | 0.098 | 0.010 | 1.71 | 5.17 | 0.18 | 0.21 | 0.98 | 0.186 |
| 11 | 0.075 | 0.008 | 1.52 | 4.70 | 0.18 | 0.27 | 0.96 | 0.231 |
| 12 | 0.007 | 0.001 | 0.92 | 2.09 | 0.16 | 0.44 | 0.73 | 0.382 |
| 13 | 0.032 | 0.003 | 1.22 | 2.31 | 0.19 | 0.40 | 0.81 | 0.339 |
| 14 | 0.013 | 0.001 | 0.98 | 2.18 | 0.17 | 0.42 | 0.76 | 0.363 |
| 15 | 0.111 | 0.011 | 1.84 | 5.66 | 0.18 | 0.17 | 0.98 | 0.145 |
| 16 | 0.109 | 0.011 | 1.81 | 5.60 | 0.18 | 0.17 | 0.98 | 0.148 |
| 17 | 0.095 | 0.010 | 1.68 | 5.06 | 0.18 | 0.22 | 0.97 | 0.189 |
| 18 | 0.053 | 0.005 | 1.39 | 3.54 | 0.19 | 0.33 | 0.93 | 0.286 |
| 19 | 0.108 | 0.011 | 1.80 | 5.57 | 0.18 | 0.18 | 0.98 | 0.151 |
| 20 | 0.034 | 0.003 | 1.24 | 2.36 | 0.19 | 0.38 | 0.82 | 0.332 |
| 21 | 0.082 | 0.008 | 1.58 | 4.60 | 0.18 | 0.25 | 0.96 | 0.212 |
| 22 | 0.023 | 0.002 | 1.09 | 2.24 | 0.18 | 0.41 | 0.78 | 0.354 |
| 23 | 0.087 | 0.009 | 1.62 | 4.79 | 0.18 | 0.23 | 0.97 | 0.198 |
| 24 | 0.113 | 0.011 | 1.86 | 5.72 | 0.18 | 0.16 | 0.99 | 0.139 |
| 25 | 0.114 | 0.011 | 1.87 | 5.76 | 0.18 | 0.16 | 0.99 | 0.136 |
| 26 | 0.085 | 0.009 | 1.61 | 4.72 | 0.18 | 0.24 | 0.97 | 0.203 |
| 27 | 0.002 | 0.000 | 0.86 | 2.06 | 0.16 | 0.45 | 0.67 | 0.390 |
| 28 | 0.022 | 0.002 | 1.08 | 2.23 | 0.18 | 0.41 | 0.78 | 0.355 |
| 29 | 0.019 | 0.002 | 1.05 | 2.21 | 0.18 | 0.41 | 0.77 | 0.358 |
| 30 | 0.066 | 0.007 | 1.46 | 4.32 | 0.18 | 0.30 | 0.95 | 0.258 |
| 31 | 0.105 | 0.011 | 1.78 | 5.44 | 0.18 | 0.19 | 0.98 | 0.161 |
| 32 | 0.008 | 0.001 | 0.93 | 2.10 | 0.16 | 0.43 | 0.74 | 0.379 |
| 33 | 0.096 | 0.010 | 1.69 | 5.10 | 0.18 | 0.22 | 0.97 | 0.188 |
| 34 | 0.116 | 0.012 | 1.88 | 5.82 | 0.18 | 0.16 | 0.99 | 0.131 |
| 35 | 0.052 | 0.005 | 1.39 | 3.51 | 0.19 | 0.33 | 0.92 | 0.288 |
| 36 | 0.074 | 0.007 | 1.51 | 4.67 | 0.18 | 0.27 | 0.96 | 0.234 |
| 37 | 0.005 | 0.001 | 0.89 | 2.07 | 0.16 | 0.44 | 0.70 | 0.385 |
| 38 | 0.115 | 0.012 | 1.87 | 5.79 | 0.18 | 0.16 | 0.99 | 0.133 |
| 39 | 0.080 | 0.008 | 1.56 | 4.88 | 0.18 | 0.26 | 0.96 | 0.217 |
| 40 | 0.073 | 0.007 | 1.51 | 4.63 | 0.18 | 0.28 | 0.96 | 0.236 |
| 41 | 0.012 | 0.001 | 0.97 | 2.16 | 0.17 | 0.42 | 0.76 | 0.365 |
| 42 | 0.054 | 0.005 | 1.40 | 3.58 | 0.19 | 0.32 | 0.93 | 0.282 |
| 43 | 0.046 | 0.005 | 1.35 | 3.27 | 0.19 | 0.35 | 0.87 | 0.300 |
| 44 | 0.076 | 0.008 | 1.52 | 4.71 | 0.18 | 0.27 | 0.96 | 0.230 |
| 45 | 0.106 | 0.011 | 1.78 | 5.48 | 0.18 | 0.19 | 0.98 | 0.160 |
| 46 | 0.021 | 0.002 | 1.07 | 2.22 | 0.18 | 0.41 | 0.77 | 0.356 |
| 47 | 0.083 | 0.008 | 1.59 | 4.64 | 0.18 | 0.25 | 0.97 | 0.209 |
| 48 | 0.006 | 0.001 | 0.91 | 2.08 | 0.16 | 0.44 | 0.72 | 0.384 |
| 49 | 0.049 | 0.005 | 1.37 | 3.40 | 0.19 | 0.34 | 0.89 | 0.296 |
| 50 | 0.092 | 0.009 | 1.66 | 4.94 | 0.18 | 0.22 | 0.97 | 0.189 |

Table 6 (continued)

| # | HC | NQF | Cc | Cu | w _{max} | Ip | $\sigma_{\text{part}}/\sigma_{\text{max}}$ | Ccs |
|-----------------------|-------|-------|------|------|------------------|------|--|-------|
| 51 | 0.033 | 0.003 | 1.23 | 2.32 | 0.19 | 0.39 | 0.81 | 0.335 |
| 52 | 0.004 | 0.000 | 0.88 | 2.06 | 0.16 | 0.45 | 0.69 | 0.387 |
| 53 | 0.071 | 0.007 | 1.49 | 4.54 | 0.18 | 0.29 | 0.96 | 0.244 |
| 54 | 0.100 | 0.010 | 1.73 | 5.24 | 0.18 | 0.21 | 0.98 | 0.182 |
| 55 | 0.079 | 0.008 | 1.55 | 4.84 | 0.18 | 0.26 | 0.96 | 0.221 |
| 56 | 0.014 | 0.001 | 0.99 | 2.19 | 0.17 | 0.42 | 0.76 | 0.362 |
| 57 | 0.081 | 0.008 | 1.57 | 4.56 | 0.18 | 0.26 | 0.96 | 0.215 |
| 58 | 0.099 | 0.010 | 1.72 | 5.20 | 0.18 | 0.21 | 0.98 | 0.184 |
| 59 | 0.026 | 0.003 | 1.13 | 2.27 | 0.18 | 0.41 | 0.79 | 0.349 |
| 60 | 0.103 | 0.010 | 1.76 | 5.38 | 0.18 | 0.20 | 0.98 | 0.172 |
| 61 | 0.000 | 0.000 | 0.84 | 2.05 | 0.16 | 0.45 | 0.65 | 0.392 |
| 62 | 0.055 | 0.006 | 1.41 | 3.65 | 0.19 | 0.32 | 0.94 | 0.280 |
| 63 | 0.057 | 0.006 | 1.42 | 3.76 | 0.19 | 0.32 | 0.94 | 0.277 |
| 64 | 0.031 | 0.003 | 1.21 | 2.30 | 0.19 | 0.40 | 0.80 | 0.342 |
| 65 | 0.064 | 0.006 | 1.46 | 4.20 | 0.18 | 0.30 | 0.95 | 0.260 |
| 66 | 0.058 | 0.006 | 1.42 | 3.80 | 0.19 | 0.32 | 0.95 | 0.276 |
| 67 | 0.118 | 0.012 | 1.89 | 5.53 | 0.17 | 0.15 | 0.99 | 0.125 |
| 68 | 0.088 | 0.009 | 1.63 | 4.80 | 0.18 | 0.23 | 0.97 | 0.195 |
| 69 | 0.017 | 0.002 | 1.03 | 2.20 | 0.17 | 0.41 | 0.77 | 0.360 |
| 70 | 0.039 | 0.004 | 1.27 | 2.52 | 0.19 | 0.37 | 0.84 | 0.324 |
| 71 | 0.112 | 0.011 | 1.85 | 5.69 | 0.18 | 0.17 | 0.98 | 0.142 |
| 72 | 0.018 | 0.002 | 1.04 | 2.20 | 0.18 | 0.41 | 0.77 | 0.360 |
| 73 | 0.009 | 0.001 | 0.94 | 2.12 | 0.16 | 0.43 | 0.74 | 0.375 |
| 74 | 0.110 | 0.011 | 1.83 | 5.63 | 0.18 | 0.17 | 0.98 | 0.147 |
| 75 | 0.048 | 0.005 | 1.36 | 3.36 | 0.19 | 0.35 | 0.89 | 0.299 |
| 76 | 0.038 | 0.004 | 1.27 | 2.45 | 0.19 | 0.38 | 0.83 | 0.326 |
| 77 | 0.001 | 0.000 | 0.85 | 2.05 | 0.16 | 0.45 | 0.66 | 0.392 |
| 78 | 0.084 | 0.008 | 1.60 | 4.69 | 0.18 | 0.24 | 0.97 | 0.205 |
| 79 | 0.051 | 0.005 | 1.38 | 3.49 | 0.19 | 0.34 | 0.92 | 0.291 |
| 80 | 0.061 | 0.006 | 1.43 | 3.98 | 0.19 | 0.31 | 0.95 | 0.270 |
| <i>Validation set</i> | | | | | | | | |
| 81 | 0.101 | 0.010 | 1.74 | 5.28 | 0.18 | 0.21 | 0.98 | 0.180 |
| 82 | 0.107 | 0.011 | 1.79 | 5.53 | 0.18 | 0.19 | 0.98 | 0.157 |
| 83 | 0.086 | 0.009 | 1.61 | 4.76 | 0.18 | 0.24 | 0.97 | 0.202 |
| 84 | 0.077 | 0.008 | 1.53 | 4.75 | 0.18 | 0.26 | 0.96 | 0.227 |
| 85 | 0.056 | 0.006 | 1.41 | 3.70 | 0.19 | 0.32 | 0.94 | 0.279 |
| 86 | 0.037 | 0.004 | 1.25 | 2.43 | 0.19 | 0.38 | 0.83 | 0.327 |
| 87 | 0.040 | 0.004 | 1.28 | 2.59 | 0.19 | 0.37 | 0.84 | 0.322 |
| 88 | 0.069 | 0.007 | 1.48 | 4.48 | 0.18 | 0.29 | 0.96 | 0.246 |
| 89 | 0.091 | 0.009 | 1.65 | 4.92 | 0.18 | 0.22 | 0.97 | 0.189 |
| 90 | 0.010 | 0.001 | 0.95 | 2.14 | 0.17 | 0.42 | 0.75 | 0.371 |
| 91 | 0.024 | 0.002 | 1.10 | 2.25 | 0.18 | 0.41 | 0.78 | 0.353 |
| 92 | 0.117 | 0.012 | 1.88 | 5.82 | 0.17 | 0.16 | 0.99 | 0.130 |
| 93 | 0.050 | 0.005 | 1.38 | 3.45 | 0.19 | 0.34 | 0.90 | 0.294 |
| 94 | 0.025 | 0.003 | 1.12 | 2.26 | 0.18 | 0.41 | 0.79 | 0.350 |
| 95 | 0.047 | 0.005 | 1.35 | 3.31 | 0.19 | 0.35 | 0.88 | 0.299 |
| 96 | 0.044 | 0.004 | 1.33 | 2.96 | 0.19 | 0.35 | 0.86 | 0.305 |
| 97 | 0.035 | 0.004 | 1.24 | 2.41 | 0.19 | 0.38 | 0.82 | 0.329 |
| 98 | 0.029 | 0.003 | 1.18 | 2.29 | 0.19 | 0.40 | 0.80 | 0.344 |
| 99 | 0.027 | 0.003 | 1.15 | 2.27 | 0.18 | 0.41 | 0.79 | 0.348 |
| 100 | 0.094 | 0.009 | 1.67 | 5.01 | 0.18 | 0.22 | 0.97 | 0.189 |

Table 6 (continued)

| # | HC | NQF | Cc | Cu | w _{max} | Ip | $\sigma_{\text{part}}/\sigma_{\text{max}}$ | Ccs |
|-----|-------|-------|------|------|------------------|------|--|-------|
| 101 | 0.072 | 0.007 | 1.50 | 4.59 | 0.18 | 0.28 | 0.96 | 0.240 |
| 102 | 0.036 | 0.004 | 1.25 | 2.42 | 0.19 | 0.38 | 0.82 | 0.328 |
| 103 | 0.060 | 0.006 | 1.43 | 3.92 | 0.19 | 0.31 | 0.95 | 0.273 |
| 104 | 0.093 | 0.009 | 1.67 | 4.98 | 0.18 | 0.22 | 0.97 | 0.189 |
| 105 | 0.063 | 0.006 | 1.45 | 4.15 | 0.19 | 0.30 | 0.95 | 0.264 |
| 106 | 0.062 | 0.006 | 1.44 | 4.08 | 0.18 | 0.31 | 0.95 | 0.268 |
| 107 | 0.042 | 0.004 | 1.31 | 2.74 | 0.19 | 0.36 | 0.85 | 0.314 |
| 108 | 0.102 | 0.010 | 1.75 | 5.34 | 0.18 | 0.20 | 0.98 | 0.179 |
| 109 | 0.097 | 0.010 | 1.70 | 5.13 | 0.18 | 0.22 | 0.98 | 0.187 |
| 110 | 0.028 | 0.003 | 1.17 | 2.28 | 0.18 | 0.40 | 0.79 | 0.347 |
| 111 | 0.089 | 0.009 | 1.64 | 4.83 | 0.18 | 0.22 | 0.97 | 0.193 |
| 112 | 0.104 | 0.010 | 1.77 | 5.41 | 0.18 | 0.19 | 0.98 | 0.163 |
| 113 | 0.065 | 0.007 | 1.46 | 4.28 | 0.18 | 0.30 | 0.95 | 0.259 |
| 114 | 0.090 | 0.009 | 1.65 | 4.89 | 0.18 | 0.22 | 0.97 | 0.189 |
| 115 | 0.045 | 0.005 | 1.33 | 3.20 | 0.19 | 0.35 | 0.87 | 0.301 |
| 116 | 0.059 | 0.006 | 1.43 | 3.87 | 0.19 | 0.31 | 0.95 | 0.274 |
| 117 | 0.119 | 0.012 | 1.93 | 5.85 | 0.17 | 0.14 | 0.99 | 0.123 |
| 118 | 0.068 | 0.007 | 1.48 | 4.43 | 0.18 | 0.30 | 0.96 | 0.249 |
| 119 | 0.078 | 0.008 | 1.54 | 4.80 | 0.18 | 0.26 | 0.96 | 0.223 |
| 120 | 0.020 | 0.002 | 1.06 | 2.21 | 0.18 | 0.41 | 0.77 | 0.357 |
| 121 | 0.041 | 0.004 | 1.30 | 2.64 | 0.19 | 0.37 | 0.85 | 0.320 |

Appendix 2

See Table 6.

References

- Zahiri A, Hashemi F (2017) Assessment of flow discharge prediction in main channels using GEP and traditional models. *J Civ Eng Urban* 7(3):41–47
- El-Bosraty AH, Ebid AM, Fayed AL (2020) Estimation of the undrained shear strength of east Port-Said clay using the genetic programming. *Ain Shams Eng J.* <https://doi.org/10.1016/j.asej.2020.02.007>
- Alavi A, Sadrossadat E (2016) New design equations for estimation of ultimate bearing capacity of shallow foundations resting on rock masses. *Geosci Fronts.* <https://doi.org/10.1016/j.gsf.2014.12.005>
- American Standard for Testing and Materials (ASTM) C618 (1978) Specification for Pozzolanas. ASTM International, Philadelphia, USA
- American Standard for Testing and Materials (ASTM) E1621-13 (2013) Standard guide for elemental analysis by wavelength dispersion x-ray fluorescence spectrometry, ASTM International, West Conshohocken, PA. doi: <https://doi.org/10.1520/E1621-13>
- Selle B, Muttill N (2011) Testing the structure of a hydrological model using genetic programming. *J Hydrol.* <https://doi.org/10.1016/j.jhydrol.2010.11.009>
- BS 1377–2,3 (1990) Methods of testing soils for civil engineering purposes, British Standard Institute, London
- BS 1924 (1990) Methods of tests for stabilized soil, British Standard Institute, London
- Ebid AM (2004) Applications of genetic programming in geotechnical engineering, Ph.D. Thesis, Ain Shams University, Cairo, Egypt, <https://doi.org/10.13140/RG.2.1.1967.9203>
- Edjabou ME, Martín-Fernández JA, Scheutz C, Astrup TF (2017) Statistical analysis of solid waste composition data: arithmetic mean, standard deviation and correlation coefficients. *Waste Manage* 69:13–23
- Gandomi AH, Alavi AH (2013) Expression programming techniques for formulation of structural engineering systems. In: Gandomi H, Yang X, Talatahari S, Alavi H (eds) *Metaheuristic applications in structures and infrastructures*, pp. 437–454. Elsevier Science, New York. <https://doi.org/10.1016/B978-0-12-398364-0.00018-8>
- Canakci H, Baykasoglu A, Güllü H (2009) Prediction of compressive and tensile strengths of Gaziantep basalts via neural network and Gene expression programming. *Neural Comput Appl.* <https://doi.org/10.1007/s00521-008-0208-0>
- Azamathulla H, Zahiri A (2012) Flow discharge prediction in compound channels using linear genetic programming. *J Hydrol.* <https://doi.org/10.1016/j.jhydrol.2012.05.065>
- Pérez J, Miguélez M, Rabuñal J, Abella F (2008) Applying genetic programming to civil engineering in the improvement of models, codes and norms, conference paper, https://doi.org/10.1007/978-3-540-88309-8_46
- Onyelowe KC, Jalal FE, Onyia ME, Onuoha IC, Alaneme GU (2021) Application of gene expression programming to evaluate strength characteristics of hydrated-lime-activated rice husk ash-treated expansive soil. *Appl Comput Intell Soft Comput.* <https://doi.org/10.1155/2021/6686347>
- Onyelowe KC, Iqbal M, Jalal FE (2021) Smart computing models of California bearing ratio, unconfined compressive strength, and resistance value of activated ash-modified soft clay soil with adaptive neuro-fuzzy inference system and ensemble random

- forest regression techniques. *Multiscale Multidiscipl Model Exp Des*. <https://doi.org/10.1007/s41939-021-00092-8>
17. Onyelowe KC, Iqbal M, Jalal FE, Onyia ME, Onuoha IC (2021) Application of 3-algorithm ANN programming to predict the strength performance of hydrated-lime activated rice husk ash treated soil. *Multiscale Multidiscipl Model Exp Des*. <https://doi.org/10.1007/s41939-021-00093-7>
 18. Onyelowe KC, Onyia ME, Van Bui D, Baykara H, Ugwu HU (2021) Pozzolanic reaction in clayey soils for stabilization purposes: a classical overview of sustainable transport geotechnics. *Adv Mater Sci Eng*. <https://doi.org/10.1155/2021/6632171>
 19. Koza JR (1992) (1992) Genetic programming: on the programming of computers by means of natural selection. The MIT Press, Cambridge
 20. Mazari M, Rodriguez D (2016) Prediction of pavement roughness using a hybrid gene expression programming-neural network technique. *J Traff Transp Eng*. <https://doi.org/10.1016/j.jtte.2016.09.007>
 21. Rezaia M, Javadi A (2007) A new genetic programming model for predicting settlement of shallow foundations. *Can Geotech J*. <https://doi.org/10.1139/T07-063>
 22. Benbouras M, Mitiche R, Zedira H, Petrisor A, Mezouar N, Debiche F (2018) A new approach to predict the compression index using artificial intelligence methods. *Mar Georesour Geotechnol*. <https://doi.org/10.1080/1064119X.2018.1484533>
 23. Ibrahim N, Rahim N, Amat R, Salehuddin S, Ariffin N (2012) Determination of plasticity index and compression index of soil at Perlis. *APCBEE Proc*. <https://doi.org/10.1016/j.apcbee.2012.11.016>
 24. Onyelowe KC (2021) Application of calculus of variation in the optimization of functional parameters of compacted modified soils: a simplified computational review. *Math Prob Eng*. <https://doi.org/10.1155/2021/6696392>
 25. Ranasinghe RATM, Jaksa M, Nejad P, Kuo Y-L (2017) Predicting the effectiveness of rolling dynamic compaction using genetic programming. *Proc Inst Civ Eng Ground Improv*. <https://doi.org/10.1680/jgrim.17.00009>
 26. Ranasinghe RATM, Jaksa M, Nejad P, Kuo Y-L (2019) Genetic programming for predictions of effectiveness of rolling dynamic compaction with dynamic cone penetrometer test results. *J Rock Mech Geotech Eng*. <https://doi.org/10.1016/j.jrmge.2018.10.007>
 27. Sharma C, Ojha C (2020) Statistical parameters of hydrometeorological variables: standard deviation, SNR, skewness and kurtosis. *Adv Water Resour Eng Manage*
 28. Shaw D, Miles J, Gray A (2004) Genetic programming within civil engineering. In: Parmea I (ed) *Adaptive computing in design and manufacture VI*. Springer, The Language of Science. <https://doi.org/10.1007/978-0-85729-338-1>
 29. Skempton AW (1944) Notes on the compressibility of clays. *Quart J Geol Soc Lond* 100:119–135
 30. Vidal J M, Huynh N (2010) Building agent-based models of seaport container terminals. In: *Proceedings of 6th workshop on agents in traffic and transportation*

Publisher's Note Springer Nature remains neutral with regard to jurisdictional claims in published maps and institutional affiliations.